Channel Models for Indoor UWB Short Range Communications

Xiongwen Zhao, *Senior Member IEEE*, and Suiyan Geng
School of Electrical and Electronic Engineering, North China Electric Power University
102206, Beijing, China

Abstract—**The cluster-based tapped-delay-line (TDL) models, and the novel path loss models vs. the transceiver distance and frequency band are developed in the paper. The TDL and path loss models are very useful for the UWB radio link level simulations and for the radio coverage predictions at any given distance with any frequency band.**

I. INTRODUCTION

Ultrawideband (UWB) radio is important in future short range communications, especially in indoor and rural environments for the fast traffic connections between a UWB transmitter and a computer, and among personal computers. For UWB radio system design, two models are critical. One is the path loss models for radio coverage, another is the cluster based tapped-delay-line (TDL) channel models for the link level simulations. In most of the open literature [1]-[7], path loss models are either related to the transceiver distance or the frequency band. In [2], UWB path loss models with the transceiver distances are summarized in detail from the open literature for indoor channel. However for UWB radios, path loss models related to both the distance and frequency band are do required in a specific system design and its coverage predictions.

II. MEASUREMENT SETUP AND CAMPAIGN

A. Measurement Setups

Frequency domain measurement was built by using a vector network analyzer (VNA). In the measurements, the VNA used 3200 tones to sweep a frequency band of 3-10 GHz which was segmented into two pieces of 3-6.5 GHz and 6.5-10 GHz for enhancing the delay range. The channel impulse responses were
obtained by the inverse Fourier transformation of the frequency domain measurement data. To remove the small-scale fading effect, spatial averaging was adopted, i.e., at each measurement position the measurement was performed at 25 grid points with 10 cm grid space in a square [7].

B. Measurement Campaign

Fig. 1 shows the measurement layout in a corridor. Both line-of-sight (LOS) and non-LOS (NLOS) measurements were performed. In the LOS measurements, the transmitter TX was located in the corridor with two meters away from point 1, the receiver was placed in the fixed positions from point 1 to point 12. The measurement started from point 1 and took one meter step till point 8 with the door open. Point 9 is at the same position as point 8, however, from point 9 till point 12, the door is closed and the distance step changed as two meters away from each other. The measurements were done after working hours to avoid the effect of moving people. In NLOS measurements, the transmitter was located in the room shown in Fig. 1, and the receiver is placed at different positions from point 1 to 10 by way of point 9' with one meter distance away from each other and the door closed. The distance from the transmitter to point 1 is about 5.1 meters.
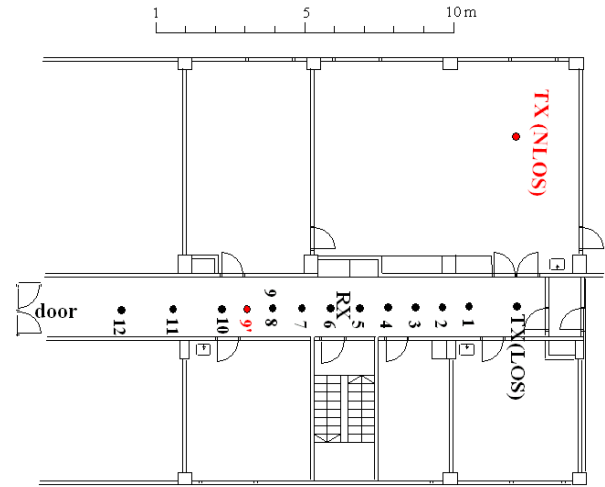

Fig. 1. Corridor Measurement layout

III. CLUSTER BASED DELAY LINE CHANNEL MODELS

The power delay profiles (PDPs) for the LOS measurements are plotted in Fig. 2(a) where the receiver is located at different positions as described in II and shown in Fig. 1. The 30 dB dynamic range is used for noise cut. From RX1 to RX8, the receiver is away from the transmitter TX(LOS) with the distances from two to nine meters, basically two clusters are observed. At RX8, one more cluster has just started to appear. RX9 is the same position as RX8, the only difference is that starting from RX9 onwards the door is closed. At RX9, three clusters can be obviously seen. The 3rd cluster is much strong compared to the one at RX8. The 2nd cluster at RX8 is now

divided into two subclusters at RX9, the two subclusters can be regarded as in one cluster due to small delay range (same as at RX10 and RX12). It's seen that UWB radio is greatly affected by the change of the environment, e.g. the cluster structures and tap powers are changed when the door is open and closed.
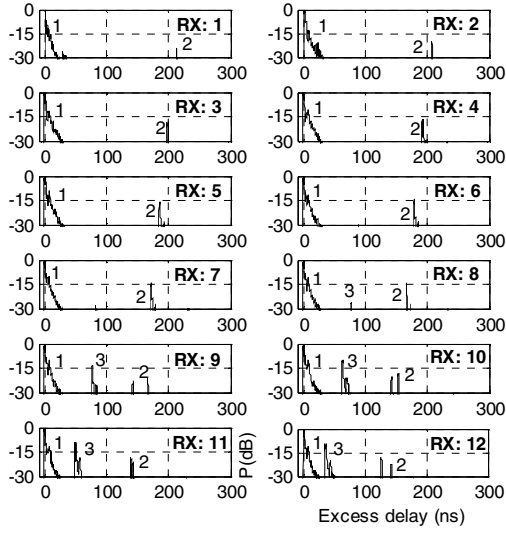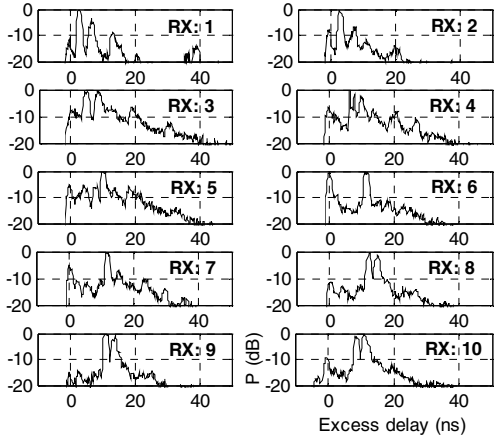

Fig. 2(a)

Fig. 2(b).
Fig. 2 The PDPs at different locations in the corridor. (a) LOS. (b) NLOS.

From Fig, 2(a), another interesting phenomenon is that the clusters (e.g. clusters 2 and 3) are moving when the distances between the transceiver are increasing. The clusters are obviously located at the side of the corridor with the door, and they follow the Saleh-Valenzuela model [8].

Table I (A) shows the cluster based TDL models for the LOS cases corresponding to the PDPs shown in Fig. 2(a). Cluster 1 is the main cluster which can contain more taps. Clusters 2 and 3 have less taps, but taps with large excess delays can be observed, which are the critical taps to affect the data transmission rate of the system. In Table I (A), the taps with * before mean that they are from the cluster 2, while with ** before, the taps are from cluster 3. With no sign before, the taps are from the main cluster. The TDL models are extracted by counting the local peaks in a cluster.

The PDPs for the NLOS measurements are plotted in Fig.

2(b) where the transmitter was located at the room and the receiver was placed from point 1 to point 10 with one meter away from each other by way of point 9'. In the NLOS environment, 20 dB dynamic range is applied for noise cut. From the NLOS PDPs, it's seen that only one cluster is found, with about 50 ns delay range. The first tap with zero excess delay is contributed by the transmission through the wall. The taps with the maximum powers are due to the diffraction from the two edges of the room door or contributed by other multipath in most of the RX positions. The NLOS TDL models are listed in Table I (B). Only the main cluster is found in the NLOS case.

IV. NOVEL PATH LOSS MODELS

Path loss models related to both the distance between the transceiver and the frequency are derived by the steps described in A and B.
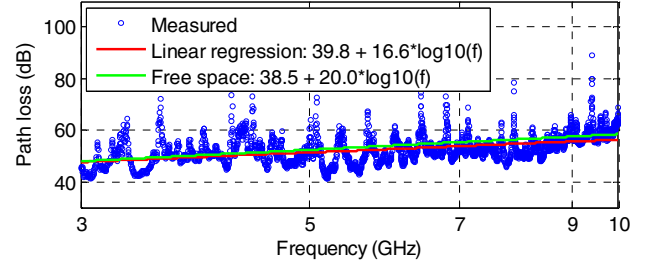

Fig. 3 Path loss and frequency band at RX1 in LOS

A. Path Loss Frequency Dependence

The path loss frequency dependences at the locations from RX1 to RX12 in the LOS, and RX1 to RX10 in the NLOS are derived first, where the linear relationship (1) is applied. As an example, Fig. 3 shows the path loss vs. frequency band at position RX1 in the LOS measurements. In (1), b is called the intercept and n the exponent, and f is in GHz. By performing the similar linear regressions at the other locations, the intercepts and 10*exponents are listed in Tables II (A) and (B) for the LOS and NLOS environments, respectively. The fitting standard deviations (stds) for the LOS and NLOS locations are within 4.9 ~6.3 dB and 5.3 ~ 6.2 dB, respectively.

$$PL = b + 10 * n * \log 10(f) \qquad (1)$$

B. Distance Dependences of the Intercept and Exponent

In Table II, the corresponding measurement distances between the transceiver are listed in the first column, the next step is to find the relationships of the intercepts and exponents with the distances. An examples, Figs. 4 (a) and (b) show the linear fittings for the intercepts and exponents for the LOS measurements. Similar ways can be applied in the NLOS case as well. The final path loss model are, therefore, related to both the distance and frequency. For LOS case, the path loss model is expressed as

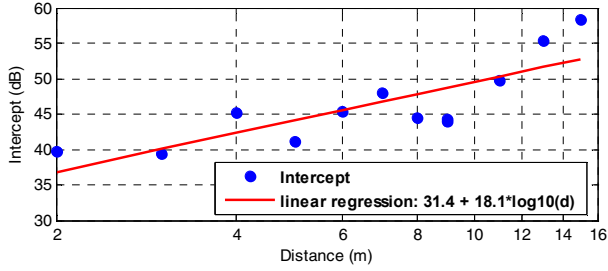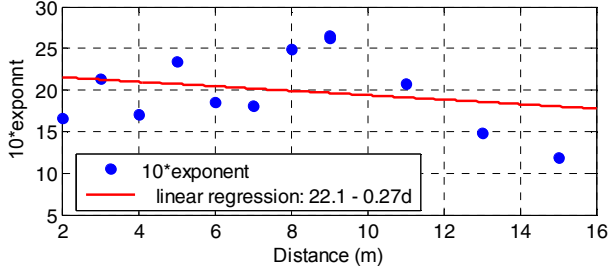$$PL = 31.4 + 18.1 * \log 10(d) + (22.1 - 0.27d) * \log 10(f) \quad (2)$$

Fig. 4 (a)

Fig. 4 (b)

Fig. 4 Relationships of the intercepts and exponents with the distances for the LOS measurements. (a) Intercept. (b) Exponent.

The distance can be in 15 meters. In the NLOS case, the path loss model can be derived as

$$PL = 28.3 + 41.9 * \log10(d) + (28.5 - 0.76d) * \log10(f) \quad (3)$$

The distance can be within 12 meters. (2) and (3) are the path loss models which are expected to be derived. However, the complicated issue is to estimate the shadow fading (SF), e.g. what are the SF standard deviations for (2) and (3) due to different fitting steps for the path loss and their related parameters. SF depends strongly on the measured environ-ments, but one measurement campaign cannot cover all the possible environments. The SF std can therefore be regarded as an empirical parameter. By open literature, the std for LOS can be within $1 - 4$ dB, and $2 - 8$ dB for NLOS environments [1][2][9]. At last, shadow fading in dB can be modeled as random variable with normal distribution with a specific standard deviation.

V. Tests of the Path Loss Models

The new models (2) and (3) are tested by using them to compare with the path loss model (1) at different receiver locations. Based on (2) and (3), the corresponding intercept and 10*exponent are tabulated in Table II as well to compare with the values obtained by (1). The fitting stds for different receiver positions are listed in the last columns in Table II (A) and (B) by using (1) and (2) for the LOS, and (1) and (3) for the NLOS, respectively. Very good agreement can be found in the most measurement locations, and the final mean stds are 1.0 and 2.0 dB for the LOS and NLOS, respectively. In [1], the path loss frequency dependence is described as f^K, where K lies in $1 - 3$ ($K = 2$ is for free space). In this work, we can find that K (exponent) lies in $1.2 - 2.7$ for the LOS and $1.1 - 3.3$ for the NLOS environments, respectively by (1)(2)(3).

TABLE II
PATH LOSS FREQUENCY FITTING. (A) LOS. (B) NOLOS

TABLE II (A)

	Path loss vs. frequency (LOS)				
	Eqn. (1)		Eqn. (2)		std (dB)
d (m)	intercept (dB)	10*exponent	intercept (dB)	10*exponent	using (1) and (2)
2	39.8	16.6	36.8	21.6	1.2
3	39.4	21.3	39.9	21.3	0.6
4	45.1	17	42.2	21	0.7
5	41.2	23.4	44	20.8	0.9
6	45.3	18.5	45.4	20.5	1.8
7	48	18.1	46.6	20.2	0.5
8	44.4	24.9	47.7	19.9	0.9
9	44.3	26.3	48.6	19.7	1.3
9	44	26.5	48.6	19.7	1.2
11	49.8	20.8	50.2	19.1	0.9
13	55.4	14.8	51.5	18.6	1
15	58.4	11.9	52.6	18.1	1.3

TABLE II (B)

	Path loss vs. frequency (NLOS)				
	Eqn. (1)		Eqn. (3)		std (dB)
d (m)	intercept (dB)	10*exponent	intercept (dB)	10*exponent	using (1) and (3)
5.08	60.6	14.9	57.9	24.6	5.2
5.41	52.1	32.8	59	24.4	1.3
5.89	63.5	23	60.6	24	2.1
6.48	63.8	23.6	62.3	23.6	1.5
7.17	63.9	21.9	64.1	23.1	1.2
7.93	69.8	12.5	66	22.5	4.3
8.73	60.7	32.3	67.7	21.9	2
9.57	77.4	10.7	69.4	21.2	1.6
10.44	65.8	25.6	71	20.6	1.4
11.33	73.3	20.6	72.5	19.9	1.4

So far, the path loss related to both the distance and frequency are derived. It's good to show how the received power changes with both of the parameters. Let's define the received power is the minus value of the path loss and no antenna gains are included. Figs. 5(a) – (c) show the received powers vs. the transceiver's distances and the frequency bands in free space, the LOS and the NLOS environments, It's seen that the received power in the LOS corridor is close the power in free space, but a bit higher power can be received due to guided wave effect. The received power in the NLOS is much lower than that in the free space and in the LOS, especially in larger distances and with higher frequencies.

VI. Conclusion

The TDL and path loss models are derived in this paper based on the corridor measurements. The TDL models are useful for the link level simulations, which is seldom to see in open literature. In most of the locations, the channel are Ricean and Rayleigh for the LOS and NLOS corridor, respectively. The traditional UWB path loss models are either distance or frequency dependence. In this paper, the new path loss models as the function of both the distance and frequency are derived, with which the UWB radio coverage can be predicted at any given distance and any interested frequency band.
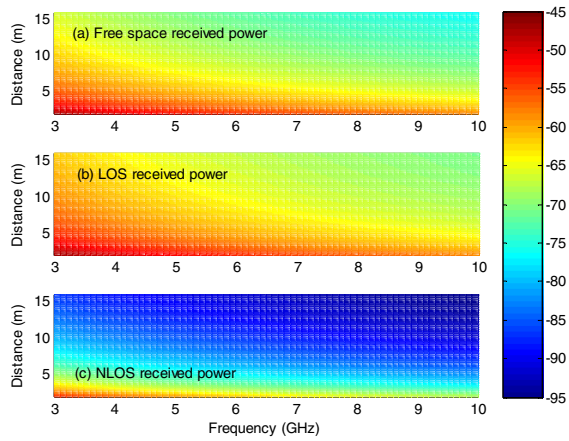
Fig.5 Path loss vs. both of the transceiver distance and frequency. (a) Free space. (b) the LOS corridor. (C) the NLOS corridor.

REFERENCES

[1] A.F. Molisch, "Ultra-Wide-Band Propagation Channels," *Proc. IEEE*, vol. 97, no. 2, pp. 353-371, Feb. 2009.

[2] B. M. Donlan, D. R. McKinstry, and R. M. Buehrer, , "The WUB Indoor Channel Large and Small Scale Modelling," *IEEE Trans. Wireless Commun.*, vol. 5, no. 10, pp. 2863-2873, Oct. 2006.

[3] S. S. Ghassemzadeh, R. Jana, C. W. Rice, W. Turin, and V. Tarokh, "Measurement and Modeling of an Ultra-Wideband Indoor Channel," *IEEE Trans. Communi.*, vol. 52, no. 10, pp. 1786- 1796, Oct. 2004.

[4] J. A. Dabin, A. M. Haimovich, and H. Grebel, "A Statistical Ultr-Wideband Indoor Channel Model and the Effects of Antenna Directivity on Path Loss and Multipath Propagation," *IEEE J. Select. Areas Communi.*, vol. 24, no. 4, pp. 752 - 758, Apr. 2006.

[5] S. Thiagarajah, B. M. Ali, and M. Ismail, "Empirical UWB Path Loss Models for Typical Office Environments," in *Proc. 13th IEEE Int. Conf. Networks*, Malaysia, vol. 2, Nov. 2005, pp. 16-18.

[6] R. Saadane, M. Wanbi, A. Hayar, and D. Aboutajdine, "Path Loss Analysis Based on UWB Channel Measurements," in *Proc. IEEE Int. Conf. Computer Systems Applications*, Rabat, Morocoo, May 10-13, 2009, pp. 970-974

[7] S. Geng, S. Ranvier, X. Zhao, J. Kivinen, and P. Vainikainen, "Multipath Propagation Characterization of Ultra-wide Band Indoor Radio Channels," in *Proc. IEEE Int. Conf. Ultra-Wideband*, Zurich, Switzerland, Sept. 5-8, 2005, pp. 11-15.

[8] A. A. M. Saleh and R. A. Valenzuela, "A statistical model for indoor multipath propagation," *IEEE J. Select. Areas Commun.*, vol. 5, pp. 128-137, Feb. 1987.

[9] *WINNER II: Channel Models*, IST-4-027756 WINNER II, D1.1.2 V1.1, 2007.

TABLE I CLUSTER BASED TAPPED DELAY LINE MODELS. (A) LOS. (B) NOLOS

RX1		RX2		RX3		RX4		RX5		RX6		RX7		RX8		RX9		RX10		RX11		RX12	
Delay (ns)	P (dB)																						
0	0	0	0	0	0	0	0	0	0	0	0	0	0	0	0	0	0	0	0	0	0	0	0
0.7	-0.8	2	-5.5	1.3	-4.9	1	-4.1	3.9	-12	3.6	-11	3.1	-8.6	3	-7.9	3	-8	1.6	-7.3	4	-14.1	3.9	-11.8
3.2	-7.1	7.7	-12.9	6.7	-11.7	7.4	-11.1	7.4	-9.4	6.6	-11.9	6.7	-9.6	6.7	-10.4	6.7	-10.3	6.7	-10.5	7.2	-11.6	7.4	-11.5
5.4	-11.4	11.7	-19.5	14.3	-17.5	4.4	-12.6	10.4	-17.4	9.7	-15.2	9.9	-16.9	11.6	-18.5	13.6	-22.3	8.4	-12.3	9.9	-18.9	**36,4	**-9,1
9	-15.5	21.9	-21.1	19.2	-23.8	12.1	-18.2	16	-20.3	12.9	-20.5	12.5	-19.3	16.6	-22.6	**76,1	**-13,5	11.3	-19.4	11.3	-21.3	**43,3	**-20,1
12	-21	25.9	-25.4	*199	*-17,9	23.4	-25.6	23.3	-26	17.4	-24.2	16.3	-22.3	*165,1	*-13,9	**83	**-25,2	15.4	-23.1	**49,2	**-9	*126,2	*-18
27.4	-26.3	*206,7	*-20,5			*192,4	*-16,3	*185,4	*-15,7	21.7	-25.9	*172	*-14,2			*142	*-23	**62,9	**-10	**56,3	**-18,6	142,9	*-22,4
*213,4	*-24							*178,7	*-14,5							*166,1	*-21,2	**70,1	**-20,8	138,1	*-18,2		
																		*142,3	*-20,6	142,4	*-21,4		
																		*152,7	*-18,6				

* The taps in the 2nd cluster. ** The taps in the 3rd cluster.

TABLE I (A)

RX1		RX2		RX3		RX4		RX5		RX6		RX7		RX8		RX9		RX10	
Delay (ns)	P (dB)																		
0	-10.6	0	-8.1	0	-7.6	0	-6.7	0	-5.8	0	-1	0	-5.4	0	-11.1	0	-15.1	0	-9.7
3	0	2.7	0	5	-0.8	6.3	0	4.4	-5.8	11.1	0	5.7	-11.4	4.4	-13.2	2.6	-14.4	4.9	-14.1
6.6	-4.2	7.3	-6.7	8.3	0	7.7	-1.7	7.9	-6.2	17.7	-11	11.7	0	8.9	-12.9	11	0	8.6	-1.7
13.4	-9.2	11.3	-11.5	12.6	-5.9	10.2	-2.7	10	0	22.9	-12.9	16	-7.8	12.7	0	14.2	-1.7	10.9	0
20.9	-17.1	14.3	-15.4	19	-6.4	13.4	-7.4	13.7	-6.4	28.9	-16.4	24.1	-10.4	15	-1.4	17.3	-11.5	19.2	-12.2
38.7	-14.5	19.7	-13.6	31.2	-12.3	20.7	-8.6	18.3	-5.7	33.3	-17.7	29.7	-13.7	17.9	-10.3	25.4	-14.3	32	-18.1
		23.9	-19.4	48.3	-19.2	26.4	-10.5	22.2	-8.5			35.4	-16.9	22.7	-14	29.3	-19.6		
						31.9	-16.1	26.7	-13.3					29.4	-17				
						42.9	-19.6	32.9	-14					36.7	-19.1				
								43.9	-19.3										

TABLE I (B)